JURNAL SYNTAX TRANSFORMATION

Volume 6, No. 1 January, 2025
p-ISSN 2721-3854 | e-ISSN 2721-2769

Vapor-Liquid Equilibrium Data for The Binary Systems of Methacrylic Acid, Methyl Methacrylate, and Water at 26 kPa and 50 kPa

Zauziah Pramiswari Putri
Shandong University of Science and Technology, Qingdao, China
Email: zauziahpp@gmail.com

ABSTRACT

Methyl methacrylate (MMA) is a significant organic compound utilized across diverse industrial sectors. This research study aims to examine the separation of azeotropic systems containing MMA derived from the C4 route. The primary focus of this examination is on vapor-liquid equilibrium (VLE) data for binary systems of methacrylic acid (MAA) and water, as well as methacrylic acid and MMA. The study will be conducted under vacuum pressures of 26 kPa and 50 kPa. The objective of this study is to generate and analyze VLE data, thereby facilitating a comprehensive understanding of the azeotropic behavior and non-ideal interactions in these systems. The VLE data were obtained using a modified Rose-Williams type recirculation still. The azeotropic composition of the methacrylic acid and water system was confirmed, and the data were validated through Herrington and van Ness methods to ensure thermodynamic consistency. The findings indicate that the excess of the calculated Gibbs free energy and activity coefficient substantiates the non-ideal behavior. In conclusion, this study provides valuable insights into the design and optimization of the MMA by-product separation process. To further refine the model and enhance its predictive capabilities, additional research is recommended, focusing on exploring the impact of diverse experimental conditions and evaluating the efficacy of alternative predictive models.

Keywords: vapor-liquid equilibrium; methyl methacrylate; methacrylic acid; water; azeotrope; vacuum.

INTRODUCTION

As a highly significant and practical chemical monomer for polymerization, methyl methacrylate (MMA) is widely used in the production of plastics, poly methyl methacrylate (PMMA, organic glass), surface coatings, and adsorbents, shockproof modifiers for polyvinyl chloride, and even membrane and additives with methacrylic polymers finding widespread applications in industries such as construction, automotive, and lighting due to their exceptional transparency, durability, and weather resistance (Wang et al., 2023; Zou et al., 2022).

China is the second country in the world to have MMA technology, which is the first to achieve an advanced level on the global scale. At December 2017, the first set of 50,000 tons/year industrial equipment was finished and placed into use at Huayi Yuhuang, Dongming, Shandong Province. It has been operating at peak efficiency and productivity for one and a half years and has generated significant financial gains. Global emphasis on the annual demand and production of MMA has increased because to its high profit margins and economic prosperity

(Chen et al., 2020; Farooq et al., 2023). This reflects the growing emphasis on optimizing production processes to meet rising global demand while ensuring sustainability.

Common adopted process to produce MMA is acetone cyanohydrin (ACH) method (C3 process), ethylene-based route, and isobutene selective oxidation pathway. The pathway, used by several firms, the largest of which is ICI in 1937, and accounting for around 80% of the world's MMA output. Although until 1982 the ACH method was the only industrial process to generate MMA, there are still some issues, such as a shortage of hazardous hydrogen cyanide and the release of significant amounts of ammonium bisulfate waste.

Therefore, the ACH technology is being gradually replaced by the comparably sustainable and green ethylene- and isobutene-based. The initial process consists of four steps: hydroformylation of ethylene by CO and H_2 to propanal, Mannich reaction of formaldehyde and propanal to methylacrolein, selective oxidation of methylacrolein to methacrylic acid (MAA), and finally esterification with methanol. The more recent technology includes esterifying MAA with methanol as well as the two-step selective oxidation of isobutene to methacrolein and then to MAA (Wang et al., 2019; Wang & Cai, 2021; Zhao et al., 2020).

The oxidation of isobutylene (IB) to methacrolein (MAL), followed by the oxidation of MAL to methacrylic acid (MAA) and the esterification of MAA with methanol, are crucial steps in MMA production, with improving MAA yield being a key research focus. In recent years, research has focused on optimizing each of these reaction steps to improve conversion efficiency and catalyst selectivity oxidizing MAL due to its active α-methyl groups. Zhou *et al.* (Zhou et al., 2015, 2017) addressed this by developing a highly active oxidation catalyst using heteropoly salts of phosphomolybdic acid and phosphomolybdovanadic acid, optimizing active species, catalyst structures, and loading methods. Advanced catalytic systems, including the use of heteropoly acids and molybdenum-bismuth (Mo-Bi) composite oxides, have proven effective in significantly improving conversion rates and enhancing product selectivity. This type of catalyst is often coupled with a fixed bed reactor (Yuyu et al., 2022).

Since hydrogen cyanide (HCN) is not present in the ACH approach, the i-C4 pathway was developed commercially by enterprises in Japan where it was not feasible to anticipate a new source of HCN. In order to increase the conversion ratios and selectivity of reactions, some Japanese businesses are currently working to create new technologies, such as new catalysts. Today, the i-C4 route accounts for more than half of MMA manufacturing capacity in Japan. Direct oxidation plants are also operating in Korea, Singapore, and Thailand along with to those in Japan. Isobutylene or tert-butyl alcohol (TBA) are the raw materials used in direct oxidation methods, while methacrylic acid (MAA), which is created by a two-step oxidation reaction, is converted into MMA by esterification. The two-step and three-step methods are both used in the IB oxidation process. The three-step process includes three reactions: the oxidation of IB to methacrolein (MAL), the oxidation of MAL to methacrylic acid (MAA), and the esterification of MAA with methanol (MeOH) to produce MMA. MAA corrodes equipment, which increases the price of the equipment (Diao et al., 2015). The reaction equations are explained as follows:

$CH_2=C–(CH_3)_2$ (or $(CH_3)_3C–OH$) + $O_2 \rightarrow CH_2=C(CH_3)–CHO + H_2O$

$CH_2=C(CH_3)–CHO + \frac{1}{2}O_2 \rightarrow CH_2=C(CH_3)–COOH$

$CH_2=C(CH_3)–COOH + CH_3OH \rightarrow CH_2=C(CH_3)–COOCH_3 + H_2O$

The two-step process entails two reactions: the first step is also the oxidation of IB to MAL under oxygen atmosphere; and the second step is direct oxidative esterification of MAL with MeOH to MMA under oxygen atmosphere. This method is environmentally friendly, free of pollutants and acidic effluent, and it also has a high atom usage efficiency. Acid corrosion concerns are avoided throughout this process (Diao et al., 2015). The direct oxidative esterification method is a brand-new, environmentally responsible way to make MMA because it does not produce any toxic byproducts like ammonium bisulfate or acidic wastewater (Diao et al., 2013). The equation is explained as follows:

$CH_2 = C(CH_3)_2 + O_2 \rightarrow CH_2 = C(CH_3) – CHO + H_2O$

$CH_2 = C(CH_3) – CHO + ½\ O_2 + CH_3OH \rightarrow CH_2 = C(CH_3) – COOCH_3 + H_2O$

Methacrylic acid (MAA) is a crucial monomer in the production of polymers and is extensively utilized in contemporary engineering and industry, pharmaceuticals (Cucuruz et al., 2016), chromatographic analysis (Lin et al., 2015), and other fields (Yinge et al., 2017). However, the separation research of MAA, MAA generated by MAL oxidation is extracted from the reactor in the form of gas phase. In industry, water spray absorption is mostly used to absorb the MAA product. The MAA content in the absorption liquid is about 10-30*wt* %, Since MAA forms an azeotrope with water and has strong polarity, and the molecular interaction with water is very strong, the process of purifying MAA from dilute solutions has problems of high energy consumption and secondary pollution. Since the boiling point of MAA is higher than that of water, direct distillation separation of MAA requires the vaporization of a large amount of water (Junping, 2018). Advanced techniques like extractive distillation, azeotropic distillation, pervaporation, liquid-liquid extraction, and pressure-swing distillation can improve efficiency, offering potential energy and cost savings for azeotropic mixtures (Mahdi et al., 2015; Pilar Cumplido et al., 2023; Zhang et al., 2024).

The oxidation of MAL to MAA is key but challenging due to MAL's high reactivity. Selecting appropriate catalysts, notably Mo-P and Mo-V-P acids, is vital to enhance selectivity and conversion rates (Yuyu et al., 2022). Furthermore, heating MAL mixtures can lead to polymerization, wasting valuable MAL monomers. Various separation methods have been studied, including the absorption method using ethanol as the absorbent, and the extractive distillation absorption method using water as the absorbent method, the four-tower combined method of water washing-methanol drying-methanol absorption-recovery distillation, ionic liquid absorption method, *etc*. The ethanol absorption method first uses ethanol to absorb MAL, and then uses water as the extractant for extractive distillation. However, water and MAL form an azeotrope, which cannot meet the requirements for MMA production. To address this, accurate Vapor-Liquid Equilibrium (VLE) data is essential for optimizing distillation and

separation processes, reducing energy usage, and minimizing the environmental footprint of MMA production. Despite significant progress, there remains a lack of comprehensive VLE data for complex systems involving MAA, MMA, water, and other reaction byproducts.

This study aims to generate and analyze VLE data for the system comprising methacrylic acid (MAA), methyl methacrylate (MMA) and water, focusing on the conditions under which azeotropic behavior occurs. The goal is to provide detailed thermodynamic data that can inform the design of more efficient separation processes, particularly for systems where direct distillation is energy-intensive due to azeotrope formation. By employing state-of-the-art experimental techniques such as gas chromatography (GC) and leveraging established methodologies for VLE measurement, this research seeks to improve the separation efficiency of MAA in MMA production. In addition to generating experimental VLE data, this study will evaluate the performance of predictive models like the NRTL (Non-Random Two-Liquid).

RESEARCH METHODS

Chemicals

The chemical analytical reagents used were methacrylic acid and methyl methacrylate is commercially available. Pure water is adopted in this work, and the suppliers provided the qualities of all reagents. Table 1 gives detailed information about the CAS number, suppliers, mass fraction and boiling temperature of pure compounds at atmospheric pressure.

Table 1. Detailed information of chemicals in the experiment

Component	CAS	Suppliers	Mass Fraction	T_a/K[a]		Analysis Method
				exp at 26 kPa	exp at 50 kPa	
Methacrylic acid	79-41-4	Shanghai Macklin Biochemical Co., Ltd.	0.99	394.05	412.15	Gas Chromatography
Methyl methacrylate	80-62-6	Shanghai Macklin Biochemical Co., Ltd.	0.995	333.95	351.45	Gas Chromatography
Water	7732-18-5	Manufactured from the laboratorium	0.99	338.95	354.45	Gas Chromatography

Equipment and procedures

The VLE data for the binary systems (methacrylic acid + water) and (methyl methacrylate + methacrylic acid) were measured under vacuum pressure at 26 kPa and 50 kPa using a modified Rose-Williams type circulating still (Yan et al., 2011). During the measurement, the liquid phase and the condensate of vapor phase were recirculated to ensure sufficient contact of the liquid and vapor phases. When the equilibrium temperature was maintained stable for 40 minutes, the equilibrium temperature was recorded using a mercury temperature with accuracy

±0.1 K (Yan et al., 2011). Then the liquid and vapor phase samples were withdrawn by micro-syringe for analysis. Wsater circulating vacuum pump and U-shaped differential manometer also used in this work because the experiment conducted under vacuum pressure.

Analysis

The vapor and liquid equilibrium compositions were detected by Gas Chromatography (GC9790Plus, Fuli analytical instrument co., Ltd, China) equipped with KB-FFAP (30m*0.32mm*0.5μm) capillary column and Flame Ionization Detector (FID). Calibration curves were obtained by producing chromatograms for a set of solutions of known compositions. The peak area of each component was correlated with the corresponding mass. Hydrogen was used as carrier gas with a flow rate of 50 mL min^{-1}. The GC operating conditions are described in Table 2. In order to obtain valid data, an electronic balance, uncertainty of 0.0001 g, was used to configure five standard samples, which have known compositions and cover the entire range of systems. According to the results, the peak area of the GC was corrected. Then, all the liquid and vapor samples were measured at least three times to make the deviation less than 0.001.

Table 2. The analysis conditions for the gas chromatography

Name	Characteristic	Description
Column	Type	Capillary column
	Specification	KB-FFAP (30m*0.32mm*0.5μm)
Carrier gas	Type	Hydrogen
	Flow rate	50 ml/min
Injector	Temperature	170°C
Oven	Temperature	160°C
Detector	Type	Flame ionization detector (FID)
	Temperature	190°C

RESULTS AND DISCUSSION

Experimental Results

The isobaric VLE data for binary systems of methacrylic acid + watermethacrylic acid + methyl methacrylate at 26 kPaand 50 kPa are presented in Table 2. Meanwhile, the values of activity coefficient (γ) and excess Gibbs energy (G^E) are also shown in Table 2. The corresponding *T-x-y* phase diagrams for the above mentioned binary systems are plotted in Fig. 1-4.

Table 3. Experimental VLE results for systems of water (1) + methacrylic acid (2) at 26 kPa, water (1) + methacrylic acid (2) at 50 kPa,methacrylic acid (1) +methyl methacrylate (2) at 26 kPa, andmethacrylic acid (1) +methyl methacrylate (2) at 50 kPa.

T/K	x_1	y_1	γ_1	γ_2	G_E
water (1) + methacrylic acid (2) at 26 kPa					
338.55	1.000	1.000	1.020	13.428	0.000
338.85	0.985	0.981	1.003	13.149	7.663
338.85	0.980	0.980	1.007	13.202	18.872
339.35	0.849	0.975	1.131	14.739	295.011

340.15	0.687	0.971	1.343	17.343	574.488
340.95	0,670	0.965	1.322	16.901	530.651
341.85	0.580	0.960	1.460	18.476	625.352
346.05	0.460	0.935	1.497	18.049	535.561
346.05	0.450	0.929	1.520	18.332	544.110
352.15	0.301	0.889	1.688	19.045	463.593
355.75	0.249	0.859	1.706	18.538	395.575
366.05	0.129	0.730	1.882	18.510	250.841
373.25	0.078	0.608	1.994	18.399	169.772
377.45	0.058	0.515	1.960	17.455	125.145
385.15	0.027	0.308	1.938	16.252	59.940
389.15	0.015	0.175	1.739	14.153	29.459
394.05	0.000	0.000	-	-	0.000
water (1) + methacrylic acid (2) at 50 kPa					
354.55	1.000	1.000	0.998	10.976	0.000
354.55	0.979	0.979	0.998	10.976	-6.637
358.25	0.578	0.945	1.409	14.927	591.127
362.65	0.419	0.915	1.588	16.118	585.615
369.55	0.277	0.855	1.735	16.535	471.158
373.45	0.226	0.817	1.766	16.265	401.244
377.45	0.178	0.771	1.838	16.375	342.408
382.45	0.128	0.719	2.009	17.196	286.442
388.45	0.087	0.618	2.083	17.039	208.748
393.45	0.059	0.520	2.201	17.380	154.985
398.05	0.040	0.418	2.261	17.306	110.752
401.45	0.029	0.337	2.267	16.972	81.976
403.65	0.025	0.279	2.038	15.049	62.385
405.55	0.017	0.218	2.214	16.155	48.285
407.45	0.010	0.144	2.351	16.962	31.761
411.85	0.000	0.000	-	-	0.000
Methacrylic acid (1) + Methyl methacrylate (2) at 26 kPa					
334.15	0.000	0.000	-	-	0.000
335.95	0.067	0.004	0.930	0.055	-16.209
337.15	0.131	0.009	0.999	0.061	-2.735
339.15	0.199	0.016	1.044	0.066	21.788
341.35	0.271	0.023	0.974	0.064	-22.272
343.65	0.342	0.033	0.976	0.067	-25.872
346.15	0.410	0.045	0.969	0.069	-38.233
348.25	0.472	0.061	1.021	0.075	26.840
351.65	0.533	0.082	1.018	0.080	26.409
355.65	0.612	0.111	0.980	0.082	-38.423
359.35	0.671	0.151	1.012	0.090	23.991

364.45	0.729	0.212	1.025	0.098	54.056
371.15	0.809	0.313	1.003	0.106	6.361
377.05	0.869	0.430	0.990	0.113	-28.715
385.15	0.940	0.652	0.988	0.126	-35.943
394.05	1.000	1.000	1.002	0.142	0.000
Methacrylic acid (1) + Methyl methacrylate (2) at 50 kPa					
351.95	0.000	0.000	-	-	0.000
353.65	0.067	0.006	1.029	0.083	3.248
355.65	0.131	0.013	1.031	0.086	9.560
357.85	0.210	0.021	0.931	0.080	-46.563
359.95	0.273	0.031	0.954	0.085	-40.085
362.45	0.332	0.044	0.988	0.092	-14.137
365.85	0.421	0.063	0.950	0.093	-66.923
367.85	0.471	0.081	0.996	0.100	-7.699
371.25	0.531	0.107	1.000	0.105	-1.338
373.65	0.579	0.139	1.071	0.117	121.936
378.85	0.672	0.191	1.012	0.119	24.829
384.45	0.731	0.272	1.049	0.132	111.214
390.15	0.811	0.361	0.998	0.135	-5.128
395.45	0.872	0.493	1.033	0.149	92.061
402.15	0.930	0.670	1.026	0.160	78.734
412.15	1.000	1.000	1.001	0.174	0.000

[a] Standard uncertainties u of T, P, x and y are u (T) = 0.35 K, u (P) = 0.35 kPa, u(x) = 0.0093, u(y) = 0.0093.

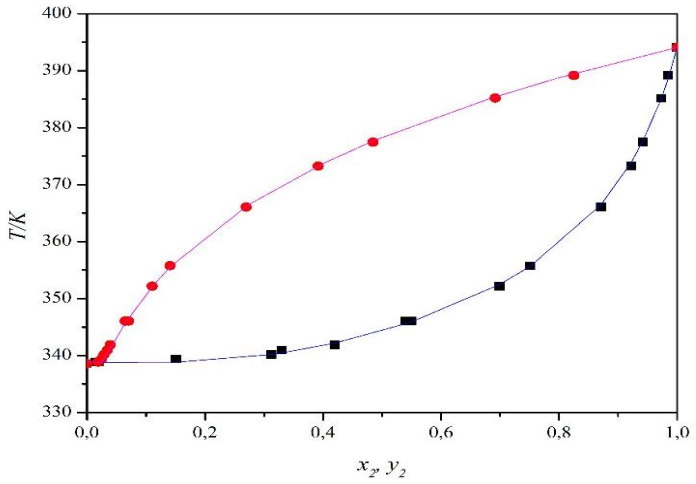

Figure 1. *T-x-y* Diagram of water (1) + MAA (2) binary system under 26 kPa: ■, T-x experimental data; ● , T-y experimental data; — , calculated by NRTL model.

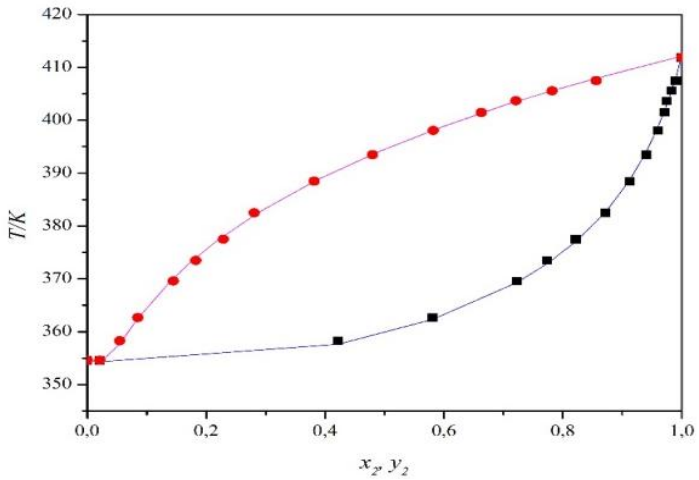

Figure 2. T-x-y Diagram of water (1) + MAA (2) binary system under 50 kPa:■ , T-x experimental data; ● , T-y experimental data;___ , calculated by NRTL model.

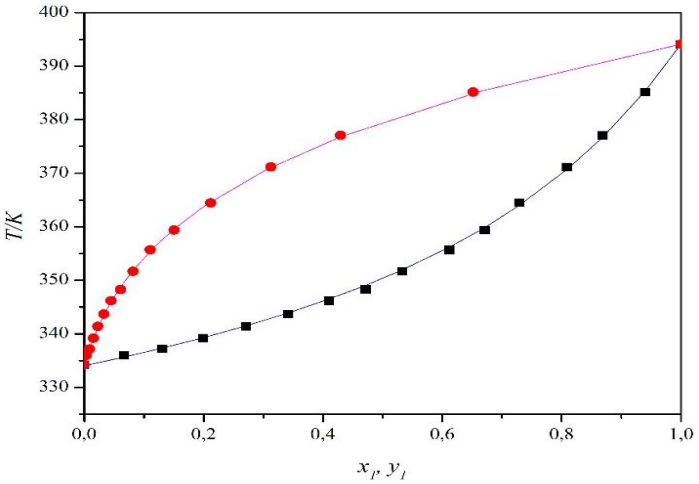

Figure 3. T-x-y Diagram of MAA (1) + MMA (2) binary system under 26 kPa:■, T-x experimental data;●, T-y experimental data; ___, calculated by NRTL model.

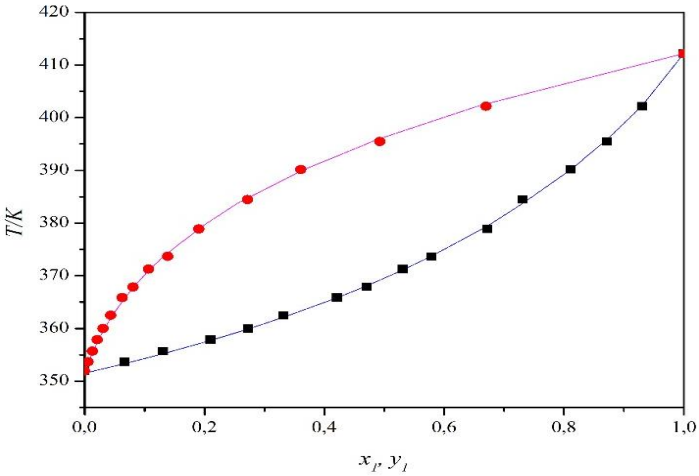

Figure 4. T-x-y Diagram of MAA (1) – MMA (2) binary system under 50 kPa:■, T-x experimental data;● , T-y experimental data;___ , calculated by NRTL model.

VLE Calculation

The equilibrium relationship between vapor phase and liquid phase can be expressed by the following equation:

$$Py_i\varphi_i = x_i\gamma_i\varphi_i^S P_i^S exp\left[\frac{V_i^L(P-P_i^S)}{RT}\right] \quad (1)$$

Where x_i and y_i are liquid and vapor mole fractions, φ_i is the fugacity coefficient of the vapor phase, φ_i^S is the saturated fugacity coefficient, $v_i^L$is the liquid molar volume, and R is the universal gas constant. The vapor phase can be assumed as ideal gas because of the low enough pressure, which leads to little interaction among molecules. Furthermore, this experiment was used under low pressure conditions, the non-ideality of steam was neglected. Thereby, where the p is not very high, it is believed that the pointing factor, φ_i and φ_i^S may be very close 1. Since, $v_i^L$is very small, (p - p_i^0) v_i^L/RT is close to 0. Then equation (3) can be simplified to the following formula:

$$\gamma_i = \frac{Py_i}{p_i^S x_i} \quad (2)$$

Where x_i and y_i are the equilibrium molar fraction of component i in liquid and vapor phase, respectively. P is the experimental pressure value, and p_i^S is the saturation vapor pressure of pure component i regarding the solution of p_i^S, the extended Antoine formula are used:

$$ln\,(P_i^S) = C_{1i} + \frac{C_{2i}}{T+C_{3i}} + C_{4i}T + C_{5i}lnT + C_{6i}T^{C_{7i}}\ C_{8i} \le T \le C_{9i} \quad (3)$$

To evaluate the non-ideality of six investigated binary systems, the excess Gibbs free energies G^E from the following equation are estimated:

$$G^E = RT\ (x_1\ ln\ \gamma_1 + x_2\ ln\ \gamma_2) \quad (4)$$

Where the activity coeffients, γ_i, were calculated from the NRTL model. From Table 2 shows that the excess Gibbs free energy for each binary system. Negative deviations from the Raoult's law were found to all binary systems. The experimental results of the relative volatilities for the components of the binary systems are shown in Fig.5. Further, the relative volatility of component i to component j, a_{ij} is defined as:

$$a_{ij} = \frac{y_i/x_i}{y_j/x_j} \quad (5)$$

Where the y and x are the molar fractions of the vapor phase and liquid phase, respectively. When the value of a_{ij} equates 1, it means that the mixture has an azeotropic point, that is, $y_i = x_i$ and $y_j = x_j$.

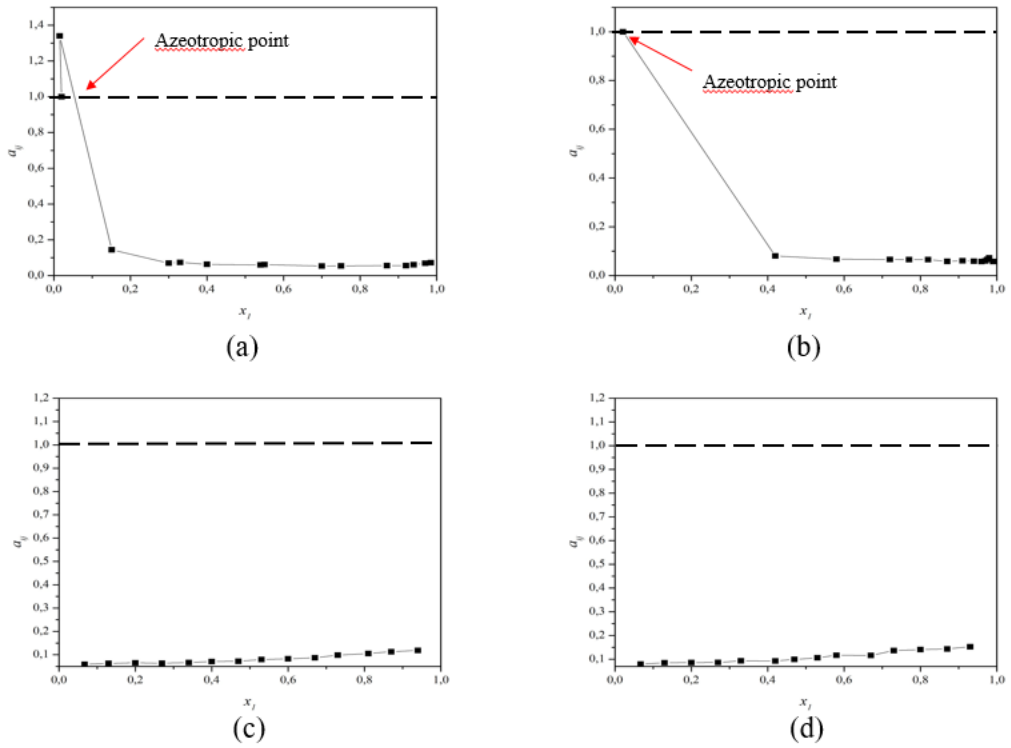

Figure 5. Diagram volatility of the (a) water + methacrylic acid at 26 kPa, (b) water + methacrylic acid at 50 kPa, (c) methacrylic acid + methyl methacrylate at 26 kPa, (d) methacrylic acid + methyl methacrylate at 50 kPa, ■ NRTL model

Thermodynamic Consistency Test

The Herington and van Ness tests were adopted to validate the thermodynamic consistency of the experimental data. Herington test were used to confirm the reliability of the measured data. The Herington test method is also called the area method, which is the integral test method of the Gibbs - Durham equation. It is a semi-empirical method used to test the reliability of the measured data. The related formula is expressed as follows:

$$D = 100\left|\frac{(A-B)}{(A+B)}\right| = 100\frac{\left|\int_0^1 ln(\gamma_1/\gamma_2)dx_1\right|}{\int_0^1 |ln(\gamma_1/\gamma_2)|dx_1} \quad (6)$$

$$J = 150\left|\frac{T_{max}-T_{min}}{T_{min}}\right| \quad (7)$$

Where, γ_1 and γ_2 are the activity coefficients calculated based on the NRTL model. *A* is represents the area enclosed by the curve above the zero horizontal axes, and *B* is represents the area enclosed by the curve below the zero horizontal axes. T_{max} is represents the highest boiling temperature, and T_{min} is represents the lowest boiling temperature. If the value of $|D-J|<10$ the Herington test can be satisfied. That is the system exhibits thermodynamic consistency.

In addition, for the measured the experimental data, van Ness test was also performed, which is a point-by-point test. This method is used to verify the reliability of the measured gas-liquid equilibrium data and calculates the average absolute deviation between the experimental data and the calculated value, so the points with large deviations can be removed. This test

requires that the values of Δy and ΔP are both less than 1, which can indicate that the measured data has passed the thermodynamic consistency test. The equation is defined as follows:

$$\Delta y = \frac{1}{N}\sum_{i=1}^{N} 100\left|y_i^{exp} - y_i^{cal}\right| \quad (8)$$

$$\Delta P = \frac{1}{N}\sum_{i=1}^{N} 100\left|\frac{P_i^{exp} - P_i^{cal}}{P_i^{exp}}\right| \quad (9)$$

Where, N is the number of experimental data points, y_i is the mole fraction of the vapor phase, and P_i is the pressure. "*Exp*" and "*cal*" represent the measurement data and calculation results of the NRTL model. The calculated Δy and ΔP are listed in Table 3 for all values, these two values are less than 1. Therefore, it is shows that the measured data by all systems have met the requirements of the van Ness test, which is, passed the thermodynamic consistency test.

Table 4. van Ness test for thermodynamic consistency check

System	Models	ΔP/kPa	Δy
MAA (1) + Water (2) at 26 kPa	NRTL	0.0657	0.5421
MAA (1) + Water (2) at 50 kPa	NRTL	0.0997	0.7759
MAA (1) + MMA (2) at 26 kPa	NRTL	0.0613	0.2175
MAA (1) + MMA (2) at 50 kPa	NRTL	0.0966	0.2971

VLE Data Correlation

The measured data results for the four binary systems of (methacrylic acid + water at 26 kPa), (methacrilic acid + water at 50 kPa), (methacrylic acid + methyl methacrylate at 26 kPa), and (methacrylic acid + methyl methacrylate at 50 kPa) were correlated using the NRTL models. The objective function is minimized according to the principle of maximum likelihood, which is expressed as follows (Jiang et al., 2019):

$$F=\sum_{i}^{N}\left[\left(\frac{P_i^{exp}-P_i^{cal}}{\sigma_P}\right)^2+\left(\frac{T_i^{exp}-T_i^{cal}}{\sigma_T}\right)^2+\left(\frac{x_i^{exp}-x_i^{cal}}{\sigma_x}\right)^2+\left(\frac{y_i^{exp}-y_i^{cal}}{\sigma_y}\right)^2\right] \quad (10)$$

Where N represents the number of the measured data, T and P are the equilibrium temperature and pressure of the binary system, and y and x are the molar fractions of component i in the vapor and liquid phases, which is refer to the standard deviation of the measured variables with 0.03 kPa for pressure, 0.1 K for temperature, and 0.001 for the vapor or liquid compositions, respectively. Summation was performed over all experimental points. The value of α_{ij} in the NRTL model was fixed to be 0.3. The superscript "*exp*" and "*cal*" represents the experimental data and the calculated value, respectively. To evaluate the difference between the experimental data and calculated results, the RMSD was calculated. The *RMSD* of vapor composition (y_1) and equilibrium temperature (T) are defined by the following equations:

$$RMSD\ (y_1) = \sqrt{\sum_{1i}^{N}\frac{\left(y_{1i}^{exp}-y_{1i}^{cal}\right)^2}{N}} \quad (11)$$

$$RMSD\ (T) = \sqrt{\sum_{1i}^{N}\frac{\left(T_i^{exp}-T_i^{cal}\right)^2}{N}} \quad (12)$$

The correlated values of the interaction parameters of RMSD are presented in Table 4. As shown in Table 4, for the four binary systems, the values of RMSD (y_1) and RMSD (T) values of each system were determined to be less than 0.0106, 0.17K, respectively.

Table 5. Regressed parameters and RMSD values for the six binary systems

Model	Parameters				*RMSD*	
	a_{ij}	a_{ji}	b_{ij}/K	b_{ji}/K	y_1 [a]	T/K [b]
			MAA (1) + Water (2) at 26 kPa			
NRTL	0.7133	2.2244	-171.993	288.8474	0.0102	0.11
			MAA (1) + Water (2) at 50 kPa			
NRTL	1.5567	9.3279	-437.34	-2328.04	0.0106	0.17
			MAA (1) + MMA (2) at 26 kPa			
NRTL	-0.08641	-0.02359	169.7897	-132.493	0.0043	0.07
			MAA (1) + MMA (2) at 50 kPa			
NRTL	4.549604	-0.91119	-1568.93	285.6157	0.0044	0.12

ABBREVIATIONS

P	total pressure, kPa
P_i^s	vapor pressure of component i, kPa
φi	fugacity coefficient of component i the vapor phase
φ_i^s	fugacity coefficient of component i at the saturated pressure
γi	activity coefficient in the liquid phase
v_i^L	liquid molar volume
xi and yi	vapor phase and liquid phase mole fractions of component i, respectively
R	universal gas constant (8.314 JK-1 mol-1)
A, B	algebraic area of ln(γ1/ γ2) vs x1
Tmax and Tmin	highesrt and the lowest boiling temperature, respectively, K
N	number of the experimental points
aij	nonrandomness parameter
exp and cal	experimental data and calculated data, respectively
T	equilibrium temperature, K
σ	standard deviation
RMSD	root-mean-square deviations

CONCLUSION

In this project, the VLE experimental results of four systems were obtained under vacuum pressure: (MAA + water at 26 kPa), (MAA + water at 50 kPa), (MAA + MMA at 26 kPa), and (MAA + MMA at 50 kPa). The thermodynamic consistency test was checked by Herington, and the van Ness test was passed for the measured binary systems. The experimental VLE data for the systems were then correlated by the NRTL model, and the values of RMSD (y1) and RMSD (T) were determined to be less than 0.0106 and 0.17K, respectively. This indicated that the correlated results show agreement with the measured VLE data. Furthermore, the binary interaction parameters of the NRTL activity coefficient model were obtained, paving the way for their application in the design, simulation, and optimization of the related separation distillation

process.Suggestions for future research include conducting further studies on the effect of variations in experimental conditions, such as temperature and pressure, on phase equilibrium. Additionally, exploring alternative prediction models beyond NRTL can enhance the precision of VLE behavior prediction in more intricate systems.In this study, VLE experimental findings were obtained for four systems: (MAA + water at 26 kPa), (MAA + water at 50 kPa), (MAA + MMA at 26 kPa), and (MAA + MMA at 50 kPa) under vacuum pressure. The thermodynamic consistency test was verified using the Herington method, and the van Ness test was successfully applied to the measured binary systems.The experimental VLE data for these systems were then correlated by the NRTL model, and the resulting RMSD (y1) and RMSD (T) values were found to be less than 0.0106 and 0.17K, respectively. This indicated that the correlated results were in agreement with the measured VLE data. Furthermore, the binary interaction parameters of the NRTL activity coefficient model were obtained, paving the way for their application in the design, simulation, and optimization of the related separation distillation process.Suggestions for future research include conducting further studies on the effect of variations in experimental conditions, such as temperature and pressure, on phase equilibrium. Additionally, exploring the use of other prediction models besides NRTL can enhance the accuracy of predicting VLE behavior in more complex systems.

BIBLIOGRAPHY

Chen, W., Fu, W., Chen, B., Peng, C., Qian, G., Chen, D., Duan, X., & Zhou, X. (2020). Polymer decoration of carbon support to boost Pt-catalyzed hydrogen generation activity and durability. *Journal of Catalysis*, *385*, 289–299. https://doi.org/10.1016/j.jcat.2020.03.023

Cucuruz, A. T., Andronescu, E., Ficai, A., Ilie, A., & Iordache, F. (2016). Synthesis and characterization of new composite materials based on poly(methacrylic acid) and hydroxyapatite with applications in dentistry. *International Journal of Pharmaceutics*, *510*(2), 516–523. https://doi.org/10.1016/j.ijpharm.2016.01.061

Diao, Y., He, H., Yang, P., Wang, L., & Zhang, S. (2015). Optimizing the structure of supported Pd catalyst for direct oxidative esterification of methacrolein with methanol. *Chemical Engineering Science*, *135*, 128–136. https://doi.org/10.1016/j.ces.2015.05.038

Diao, Y., Yang, P., Yan, R., Li, J., Wang, L., Zhang, H., Li, C., Li, Z., & Zhang, S. (2013). Deactivation and regeneration of the supported bimetallic Pd-Pb catalyst in direct oxidative esterification of methacrolein with methanol. *Applied Catalysis B: Environmental*, *142–143*, 329–336. https://doi.org/10.1016/j.apcatb.2013.04.064

Farooq, M. U., Shi, Y., Chen, W., Guan, Y., Zhou, J., Song, N., Qian, G., Zhang, J., Chen, D., Zhou, X., & Duan, X. (2023). *Kinetics insights into the active sites of Au catalysts for the oxidative*.

Jiang, S., Gao, J., Li, R., Xu, D., Zhang, L., & Wang, Y. (2019). Isobaric Vapor-Liquid Equilibrium Measurements for Separation of Azeotrope (Methanol + Methyl Acetate). *Journal of Chemical and Engineering Data*, *64*(1), 296–302. https://doi.org/10.1021/acs.jced.8b00807

Junping, Z. (2018). Simulation study on the process of coal- based methyl Methacrylate Production System. *Master Thesis, University of Chinese Academy of Sciences*.

Lin, S. L., Wu, Y. R., Lin, T. Y., & Fuh, M. R. (2015). Preparation and evaluation of poly(alkyl methacrylate-co-methacrylic acid-co-ethylene dimethacrylate) monolithic columns for separating polar small molecules by capillary liquid chromatography. *Analytica Chimica Acta*, *871*, 57–65. https://doi.org/10.1016/j.aca.2015.02.015

Mahdi, T., Ahmad, A., Nasef, M. M., & Ripin, A. (2015). State-of-the-art technologies for separation of azeotropic mixtures. *Separation and Purification Reviews*, *44*(4), 308–330. https://doi.org/10.1080/15422119.2014.963607

Pilar Cumplido, M. A., la Torre, J. De, Cerisuelo, J. P., & Chafer, A. (2023). Effect of the anion in phosphonium-based ionic liquids to recovery efficiently 2-propanol from an azeotropic mixture with water. *Fluid Phase Equilibria*, *574*(April). https://doi.org/10.1016/j.fluid.2023.113884

Wang, G., & Cai, G. (2021). Cooperative catalytic effects between Brønsted and Lewis acid sites and kinetics for production of methyl methacrylate on SO42−/TiO2-SiO2. *Chemical Engineering Science*, *229*. https://doi.org/10.1016/j.ces.2020.116165

Wang, G., Hu, X., & Zhao, S. (2023). Kinetic and thermodynamic studies on direct synthesis of methyl methacrylate from methyl propionate and methanol catalyzed by highly efficient cobalt complex at mild conditions. *Chemical Engineering Journal*, *468*.

Wang, G., Li, Z., Fan, L., Li, C., & Zhang, S. (2019). Sec-amine grafted D301 resin catalyzed fixed-bed process for continuous preparation of methacrolein via Mannich reaction. *Chemical Engineering Journal*, *370*(December 2018), 625–636. https://doi.org/10.1016/j.cej.2019.03.198

Yan, R., Li, Z., Diao, Y., Fu, C., Wang, H., Li, C., Chen, Q., Zhang, X., & Zhang, S. (2011). Green Process for Methacrolein Separation with Ionic Liquids in the Production of Methyl Methacrylate. *AIChE Journal*, *57*(9), 2388–2396. https://doi.org/10.1002/aic

Yinge, B., Yan, R., Huo, F., Qian, J., Zhang, X., & Zhang, S. (2017). Recovery of methacrylic acid from dilute aqueous solutions by ionic liquids though hydrogen bonding interaction. *Separation and Purification Technology*, *184*, 354–364. https://doi.org/10.1016/j.seppur.2017.05.013

Yuyu, S., Yiping, H., Jingjing, H., Jie, L., Xinlei, C., Yuyu, S., Yiping, H., Jingjing, H., Jie, L., & Xinlei, C. (2022). Research progress on the production of methyl methacrylate by isobutylene / tert-butanol method. *Petrochemical Technology*, *51*(11), 1342–1347. https://doi.org/10.3969/j.issn.1000-8144.2022.11.014

Zhang, Z., Peng, J., Cheng, Y., Zhang, M., Li, M., & Li, G. (2024). *Optimal design and multicriteria comparison of extractive distillation*. Separation and Purification Technology.

Zhao, H., Ran, R., Wang, L., Li, C., & Zhang, S. (2020). Novel continuous process for methacrolein production in numerous droplet reactors. *AIChE Journal*, *66*(7), 1–11. https://doi.org/10.1002/aic.16239

Zhou, L., Wang, L., Diao, Y., Yan, R., & Zhang, S. (2017). Cesium salts supported heteropoly acid for oxidation of methacrolein to methacrylic acid. *Molecular Catalysis*, *433*, 153–161. https://doi.org/10.1016/j.mcat.2017.01.023

Zhou, L., Wang, L., Zhang, S., Yan, R., & Diao, Y. (2015). Effect of vanadyl species in Keggin-type heteropoly catalysts in selective oxidation of methacrolein to methacrylic acid. *Journal of Catalysis*, *329*, 431–440. https://doi.org/10.1016/j.jcat.2015.05.031

Zou, F., Li, H., Dong, Y., Tewari, G. C., & Vapaavuori, J. (2022). Optically transparent pectin/poly(methyl methacrylate) composite with thermal insulation and UV blocking properties based on anisotropic pectin cryogel. *Chemical Engineering Journal*, *439*(December 2021), 135738. https://doi.org/10.1016/j.cej.2022.135738